Neurochemical Research (2019) 44:1653–1664
https://doi.org/10.1007/s11064-019-02791-8

ORIGINAL PAPER

Mammalian STE20-like Kinase 1 Knockdown Attenuates TNFα-Mediated Neurodegenerative Disease by Repressing the JNK Pathway and Mitochondrial Stress

Chizi Geng[1] · Jianchao Wei[1] · Chengsi Wu[1]

Received: 26 January 2019 / Revised: 28 March 2019 / Accepted: 1 April 2019 / Published online: 4 April 2019

Abstract
Neuroinflammation has been acknowledged as a primary factor contributing to the pathogenesis of neurodegenerative disease. However, the molecular mechanism underlying inflammation stress-mediated neuronal dysfunction is not fully understood. The aim of our study was to explore the influence of mammalian STE20-like kinase 1 (Mst1) in neuroinflammation using TNFα and CATH.a cells in vitro. The results of our study demonstrated that the expression of Mst1 was dose-dependently increased after TNFα treatment. Interestingly, knockdown of Mst1 using siRNA transfection significantly repressed TNFα-induced neuronal death. We also found that TNFα treatment was associated with mitochondrial stress, including mitochondrial ROS overloading, mitochondrial permeability transition pore (mPTP) opening, mitochondrial membrane potential reduction, and mitochondrial pro-apoptotic factor release. Interestingly, loss of Mst1 attenuated TNFα-triggered mitochondrial stress and sustained mitochondrial function in CATH.a cells. We found that Mst1 modulated mitochondrial homeostasis and cell viability via the JNK pathway in a TNFα-induced inflammatory environment. Inhibition of the JNK pathway abolished TNFα-mediated CATH.a cell death and mitochondrial malfunction, similar to the results obtained via silencing of Mst1. Taken together, our results indicate that inflammation-mediated neuronal dysfunction is implicated in Mst1 upregulation, which promotes mitochondrial stress and neuronal death by activating the JNK pathway. Accordingly, our study identifies the Mst1–JNK-mitochondria axis as a novel signaling pathway involved in neuroinflammation.

Keywords Mst1 · JNK pathway · Neuroinflammation · Mitochondrial stress · Apoptosis

Introduction

Neurodegenerative disease, a life-threatening nervous system disorder, affects millions of people worldwide. Parkinson's disease, Huntington's disease and Alzheimer's disease are the most common types and affect several body activities, including balance, movement, and breathing. Due to the poor regeneration of neurons, neurodegenerative disease is incurable, but treatment may help to improve symptoms and increase mobility. At the molecular level, neuroinflammation is a widely acknowledged risk factor involved in the development and progression of neurodegenerative disease [1]. In addition, central nervous system cells have been reported to be the main effector cells for neuroinflammatory procession. Excessive inflammation evokes oxidative stress via mitochondria-induced ROS overloading. Subsequently, excessive oxidative injury mediates neuronal dysfunction and death, contributing to the loss of functional cells in the central nervous system. Moreover, during the inflammation process, inflammatory cells are overactivated in immune cells and generate pro-inflammatory cytokines such as TNF-α, IL-1β, and IL-6. These inflammatory factors have been shown to play pivotal roles in neuron death. Although many studies have attempted to determine the molecular features of the initial signals of neuroinflammation, the upstream mediator of inflammation-mediated neuronal dysfunction has not been fully described.

Mammalian STE20-like kinase 1/2 (Mst1) is a primary component of the Hippo pathway that is involved in cell growth, proliferation, death and tumorigenesis. Early studies have identified Mst1 as a key regulator of cell death via modulating BCL2-related apoptosis [2]. Subsequent studies

✉ Chizi Geng
lingtao3651@sina.com

[1] Neurology Department, Beijing Luhe Hospital, Capital Medical University, Beijing, China

further demonstrated that Mst1 activation is linked to gastric cancer death [3], colorectal cancer apoptosis [4], and prostate cancer repression. In the central nervous system, Mst1 upregulation is noted in acute brain reperfusion stress [5], human Huntington's disease brain [6], and rat pilocarpine epilepsy [7]. In addition, increased Mst1 promotes neuronal dysfunction by inducing neuron death [8], disturbing mitochondria-dependent energy metabolism [9], impairing neuronal stem cell proliferation [10], and exacerbating ROS-mediated oxidative injury [11]. However, the role of Mst1 in inflammation-related neurodegenerative disease has not been reported. Notably, a recent study demonstrated that Mst1 is activated by subarachnoid hemorrhage and contributes to early brain injury by augmenting NF-κB-mediated inflammatory injury, supporting the pro-inflammatory property of Mst1 in the central nervous system [12]. Based on this, we performed experiments to determine whether Mst1 is also activated by inflammation-related neurodegenerative disease and participates in inflammation-mediated neural death.

Mitochondria have been reported to be potential downstream targets of Mst1. In hyperglycemic stress, increased Mst1 facilitates retinal pigmented epithelial cell apoptosis [13] and cardiomyocyte death [14] via inducing mitochondrial dysfunction. In addition, in gastric cancer, Mst1 overexpression is associated with tumor cell apoptosis via activating mitochondrial oxidative injury and bioenergetic disorder [15]. Moreover, mitochondrial dynamics [16], mitochondrial autophagy [17], and mitochondrial calcium balance [18] are also modulated by Mst1 in various disease models. In the present study, we explored whether Mst1 inhibition could attenuate mitochondrial stress and thus sustain neuronal survival in inflammation-related neurodegenerative disease.

JNK, a stress-activated protein kinase, responds to several endogenous and/or exogenous stressors, such as DNA breakage, oxidative stress, inflammation and infection. JNK has been implicated as a central player that affects anxiety and depression in the hippocampus [19]. In addition, in subarachnoid hemorrhage rats, JNK inhibition could attenuate early brain injury and neuronal apoptosis via repressing p53 phosphorylation and mitochondrial apoptosis activation [20]. More importantly, the relationship between JNK activation and neuroinflammation progression has been established. From a therapeutic point of view, intracellular anti-inflammatory and antioxidant pathways could be activated via downregulation of the JNK pathway in the postmortem frontal cortex of subjects with major depression [21]. From the perspective of physiology and pathology, the JNK pathway potentiates the inflammatory response by interacting with Nrf2 [22] and the NF-κB pathway [23]. Along with the well-documented regulatory effects of JNK on mitochondrial function and cell death, it is very important to illuminate whether the JNK pathway is controlled by Mst1 and then modulates mitochondrial stress and neuronal viability in the setting of neuroinflammation. Overall, the aim of our study was to explore the pathogenetic action of Mst1 in inflammation-induced neuronal death with a focus on JNK-mediated mitochondrial stress.

Materials and Methods

Cell Culture and Treatments

Mouse CATH.a cells (ATCC® CRL-11179™) were cultured in high-glucose DMEM (Gibco, Grand Island, NY, USA) containing 10% FBS (Gibco, Grand Island, NY, USA). After the cells reached 80% confluence, different doses of TNFα were added into the medium for 12 h based on a previous report [24].

Cell Viability and TUNEL Staining

MTT assay was used to observe the cellular viability. Cells were seeded onto a 96-well plate, and the MTT was then added to the medium (2 mg/mL; Sigma-Aldrich). Subsequently, the cells were cultured in the dark for 4 h, and DMSO was added to the medium. The OD of each well was observed at A490 nm via a spectrophotometer (Epoch 2; BioTek Instruments, Inc., Winooski, VT, USA) [25]. TUNEL assay, cells were fixed in 4% paraformaldehyde at room temperature for 30 min. After that, a TUNEL kit (Roche Apoptosis Detection Kit, Roche, Mannheim, Germany) was used on the slices according to the instructions. Finally, the sections were amplified to ×400; the apoptotic cells in at least 10 fields were randomly chosen. The apoptotic index was the proportion of apoptotic cells to total cells according to a previous study [26].

Flow Cytometry Analysis for ROS

Cell suspensions were collected. The liquor (50×*g*, digested two times) was collected, centrifuged for 2 min with the supernatant removed, supplemented with the ROS probe DHE, incubated at room temperature for 10 min, centrifuged, and washed with PBS [27]. The cells were resuspended by adding binding buffer (1×) in the dark; then, the cells were incubated at room temperature for 30 min and filtered with a nylon mesh (40 μm well). The ROS production was measured by fluorescence-activated cell sorting (FACS) [28].

Enzyme-Linked Immunosorbent Assay (ELISA)

Cellular glutathione (GSH), glutathione peroxidase (GPx) and SOD were measured via ELISA assay according to the

manufacturer's instructions. Cellular lactate production in the medium was measured via a lactate assay kit (#K607-100; BioVision, Milpitas, CA, USA) according to a previous study. The cancer glucose uptake rate was detected via a glucose absorption assay kit (#K606-100; BioVision) [29].

Detection of Mitochondrial Membrane Potential and mPTP Opening

Mitochondrial membrane potential was measured with JC-1 assays (Thermo Fisher Scientific Inc., Waltham, MA, USA; Catalogue No. M34152). Cells were treated with 5 mM JC-1 and then cultured in the dark for 30 min at 37 °C. Subsequently, cold PBS was used to remove the free JC-1, and DAPI was used to stain the nucleus in the dark for 3 min at 37 °C. The mitochondrial membrane potential was observed under a digital microscope (IX81, Olympus). In the mPTP opening assay, cells were cultured and then incubated with calcein-AM/$CoCl_2$ staining for 25 min at 37 °C in the dark [30]. Subsequently, the cells were washed with PBS three times to remove the free calcein-AM/$CoCl_2$. The change in fluorescence intensity was measured by a fluorescence microscope according to the previous study. Then, the mPTP opening was measured [31].

qRT-PCR

TRIzol reagent (Invitrogen; Thermo Fisher Scientific, Inc.) was used to isolate total RNA from cells. Subsequently, the Reverse Transcription kit (Kaneka Eurogentec S.A., Seraing, Belgium) was applied to transcribe RNA (1 μg in each group) into cDNA at room temperature (~25 °C) for 30 min [32]. The qPCR was performed with primers using SYBR™ Green PCR Master Mix (Thermo Fisher Scientific, Inc. cat. no. 4309155) [33]. The primers used in the present study were as follows: Mst1, forward, 5′GCGCGCAGTGCAATG TTAAAAGGGCAT 3′; reverse, 5′ACGCGTAACAGTCTA CAGCCATGGTCG 3′; and GAPDH forward, 5′GACATG CCGCCTGGAGAAAC 3′ and reverse, 5′ AGCCCAGGA TGCCCTTTAGT 3′.

Transfection

The siRNA against Mst1 and the pDC315-Mst1 vector were obtained from GenePharm (Shanghai, China). Meanwhile, transfection was performed using Lipofectamine 2000 (Invitrogen; Thermo Fisher Scientific, Inc.) following the manufacturer's instructions [34]. After 6 h, the cells were transferred to complete growth medium, and 48 h later, the cells were harvested and used for further experiments. The siRNA knockdown efficiency and overexpression efficiency were confirmed via western blotting [35].

Western Blotting

Total protein was extracted by RIPA (R0010, Solarbio Science and Technology, Beijing, China), and the protein concentration of each sample was detected with a bicinchoninic acid (BCA) kit (20201ES76, Yeasen Biotech Co., Ltd, Shanghai, China). Deionized water was added to generate 30-μg protein samples for each lane. A 10% sodium dodecyl sulphate (SDS) separation gel and concentration gel were prepared [36]. The following diluted primary antibodies were added to the membrane and incubated overnight: Bcl2 (1:1000, Cell Signaling Technology, #3498), Bax (1:1000, Cell Signaling Technology, #2772), pro-caspase3 (1:1000, Abcam, #ab13847), cleaved caspase3 (1:1000, Abcam, #ab49822), cyt-c (1:1000; Abcam; #ab90529), Tom20 (1:1000, Abcam, #ab186735), JNK (1:1000; Cell Signaling Technology, #4672), p-JNK (1:1000; Cell Signaling Technology, #9251), Mst1 (1:1000, Cell Signaling Technology, #3682) overnight at 4 °C. The membranes were washed 3 times with phosphate-buffered saline (PBS) (5 min each time), supplemented with horseradish peroxidase (HRP)-marked second antibody (1: 200, Bioss, Beijing, China), oscillated and incubated at 37 °C for 1 h. After incubation, each membrane was washed 3 times with PBS (5 min for each time) and reacted with enhanced chemiluminescence (ECL) solution (ECL808-25, Biomiga, CA, USA) at room temperature for 1 min; then, the extra liquor was removed, and the membranes were covered with preservative film [37]. Each membrane was observed with an X-ray machine (36209ES01, Qian Chen Biological Technology Co. Ltd., Shanghai, China) to visualize the protein expression. GAPDH was used as the internal references. The relative protein expression was the ratio of the grey value of the target band to the inner reference band.

Immunofluorescence

Cells were plated on glass slides in a 6-well plate at a density of 1×106 cells per well. Subsequently, cells were fixed in ice-cold 4% paraformaldehyde for 30 min, permeabilized with 0.1% Triton X-100, and blocked with 2% gelatine in PBS at room temperature [38]. The cells were then incubated with the primary antibodies: cyt-c (1:1000; Abcam; #ab90529), p-JNK (1:1000; Cell Signaling Technology, #9251), Mst1 (1:1000, Cell Signaling Technology, #3682) overnight at 4 °C. After being washed with PBS, the cells were incubated with secondary antibody and DAPI (1:1000 dilution in PBS) for 1 h at room

temperature. Images were obtained using a fluorescence microscope [39].

Statistical Analysis

All experimental data were analyzed using SPSS Statistics software 19.0 (SPSS Inc., Chicago, IL, USA, 2006). Repeated measures analysis of variance (ANOVA) was used to compare the escape latency among groups. Other data were compared using one-way ANOVA. Data are presented as the mean ± SEM. A value of $p \leq 0.05$ was considered significant.

Results

TNFα Reduces Cell Viability in CATH.a Cells via Upregulation of Mst1

To mimic the inflammation microenvironment, TNFα was added into the medium of cultured CATH.a cells. Then, cell viability was measured using the MTT assay. As shown in Fig. 1a, compared with the control group, TNFα treatment progressively reduced cell viability in a dose-dependent manner. Consistent with this observation, the cell death index, as assessed via an LDH release assay (Fig. 1b), was also increased in a dose-dependent manner after exposure to TNFα treatment. These data indicate that TNFα treatment

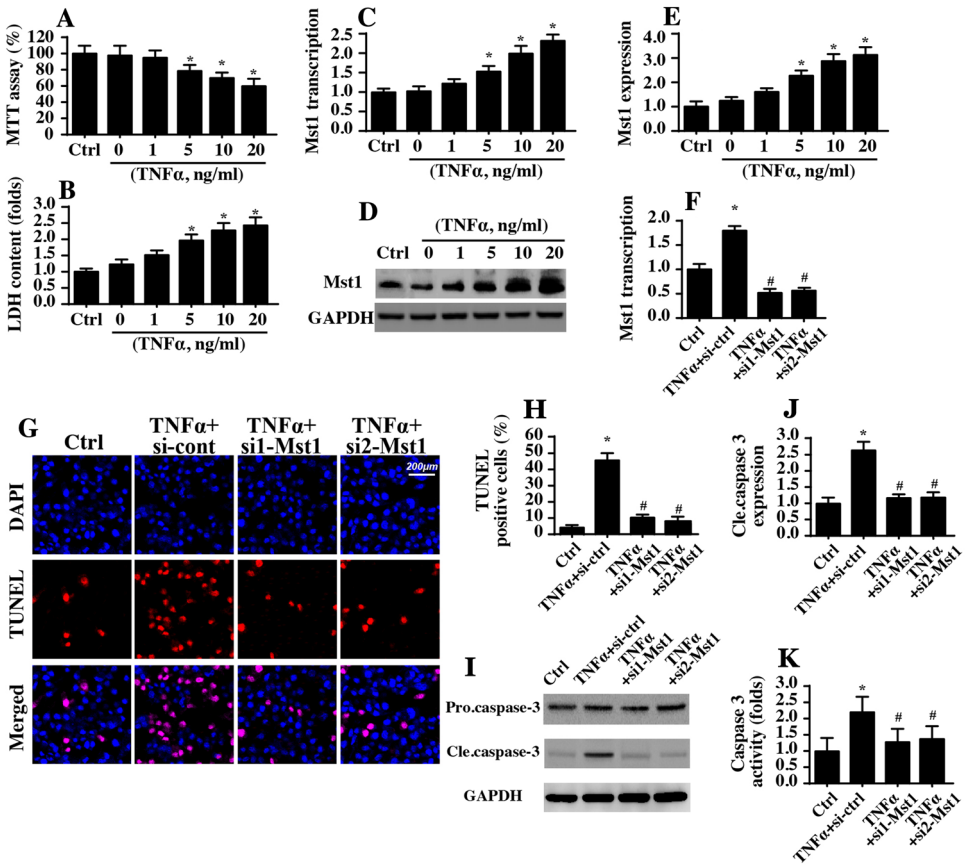

Fig. 1 Mst1 is activated by TNFα and contributes to CATH.a cell death. **a** Different doses of TNFα were added to the medium of cultured CATH.a cells, and then the viability of the cells was determined via MTT assay. **b** ELISA was used to evaluate the content of LDH in the medium, and this parameter was used to evaluate cell death in response to different doses of TNFα. **c** RNA was isolated from TNFα-treated CATH.a cells, and the transcription of Mst1 was detected. **d**, **e** Proteins were isolated from TNFα-treated CATH.a cells, and the expression of Mst1 was measured using western blot analysis. **f** TNFα-treated CATH.a cells were treated with two independent siRNAs against Mst1. Then, qPCR was used to evaluate the knockdown efficiency of each Mst1 siRNA. **g**, **h** TUNEL staining for apoptotic cells. The number of apoptotic CATH.a cells was measured in response to TNFα treatment. In addition, siRNA against Mst1 was used to knockdown Mst1 expression in TNFα-treated CATH.a cells. **i**, **j** Proteins were isolated from TNFα-treated CATH.a cells, and the expression of cleaved caspase-3 was measured using western blot analysis. **k** ELISA was used to measure the changes in caspase-3 activity. siRNA against Mst1 was used to knockdown Mst1 expression in TNFα-treated CATH.a cells. *$p < 0.05$ vs. control group; #$p < 0.05$ vs. TNFα + si-ctrl group

induces inflammatory injury in CATH.a cells. To determine the molecular mechanism by which TNFα evokes CATH.a cell damage, Mst1 transcription and expression were determined. As shown in Fig. 1c, the transcription of Mst1 was rapidly upregulated upon TNFα treatment. In addition, the expression of Mst1 was also increased in response to TNFα stress (Fig. 1d, e), indicating that inflammatory injury could be regarded as the upstream regulator of Mst1 in CATH.a cells in vitro. Considering that the minimal fatal concentration of TNFα is 5 ng/mL, this concentration was used in the following experiments. To determine whether Mst1 was involved in TNFα-mediated neuronal death, two independent siRNAs against Mst1 were transfected into CATH.a cells in vitro. The knockdown efficiency of Mst1 siRNA was confirmed via qPCR (Fig. 1f). Then, TUNEL staining was performed to observe the cell death ratio in Mst1-silenced cells. As illustrated in Fig. 1g, h, compared to the control group, TNFα markedly elevated the number of TUNEL-positive CATH.a cells, whereas Mst1 knockdown significantly repressed the rate of $TUNEL^+$ cells, indicating that Mst1 knockdown reversed CATH.a cell viability under an inflammatory microenvironment. Western blotting was used to analyze the expression of pro-apoptotic proteins. Compared with the control group, TNFα elevated the content of cleaved caspase-3 (Cle.caspase-3) in CATH.a cells (Fig. 1i, j), an effect that was accompanied by an increase in caspase-3 activity (Fig. 1k). Interestingly, loss of Mst1 prevented caspase-3 activation and upregulation, reconfirming that TNFα-mediated CATH.a cell death could be inhibited by Mst1 knockdown.

Knockdown of Mst1 Prevents TNFα-Activated Mitochondrial Apoptosis

Mitochondria, a potential downstream effector of inflammatory injury, are apoptotic triggers via the release of pro-apoptotic factors that translocate from mitochondria into the cytoplasm [40, 41]. Previous studies have found that mitochondrial apoptosis could be activated by Mst1 upregulation in a cardiac reperfusion model, in gastric cancer and in hyperglycemia-treated retinal pigmented epithelial cells [42]. In the present study, experiments were conducted to explore whether Mst1-modulated CATH.a cell death is facilitated by mitochondrial apoptosis. The first molecular feature of mitochondrial apoptosis is the release and translocation of cyt-c from mitochondria into the cytoplasm/nucleus [43]. Western blot analysis demonstrated that the expression of mitochondrial cyt-c (mito cyt-c) was rapidly reduced in response to TNFα, an effect that was accompanied by an elevation of cytoplasmic cyt-c (cyto cyt-c) and nuclear cyt-c (nuclear cyt-c) (Fig. 2a–d). Interestingly, Mst1 knockdown prevented mito cyt-c downregulation and inhibited the accumulation of cyto cyt-c and nuclear cyt-c. In addition, an immunofluorescence assay also illustrated that the expression of nuclear cyt-c was rapidly increased in TNFα-treated CATH.a cells and was reduced to near-normal levels with Mst1 knockdown (Fig. 2e, f). These results indicated that mitochondrial pro-apoptotic factor release could be repressed by Mst1 knockdown.

At the molecular level, mitochondrial permeability transition pore (mPTP) opening has been identified as a primary factor promoting mitochondrial pro-apoptotic factor release [44]. In the present study, we found that TNFα treatment elevated the opening rate of mPTP in CATH.a cells, whereas Mst1 knockdown blocked TNFα-mediated mPTP opening.

After translocating into the cytoplasm/nucleus, cyt-c activates caspase-9, and the latter elevates the activity of caspase-3 [45]. In the current study, caspase-9 activity was rapidly increased in TNFα-treated cells and was reduced to near-normal levels with Mst1 knockdown (Fig. 2h). In addition to caspase-9 activation, the level of Bax was upregulated, whereas Bcl-2 expression decreased in response to TNFα treatment (Fig. 2j, k). However, Mst1 knockdown reversed Bcl-2 expression and repressed Bax upregulation (Fig. 2j, k). Overall, the above data support that Mst1 inhibition blocked the mitochondrial apoptosis pathway in TNFα-treated CATH.a cells.

Mst1 Knockdown Maintains Mitochondrial Function in an Inflammatory Microenvironment

Next, experiments were performed to analyze the role of Mst1 in mitochondrial function under inflammatory stress. As shown in Fig. 3a, b, compared to the control group, the mitochondrial membrane potential was reduced in TNFα-treated CATH.a cells, as assessed by JC-1 staining. However, Mst1 knockdown sustained mitochondrial potential in CATH.a cells, as evidenced by the increased ratio of red-to-green fluorescence intensity (Fig. 3a, b). In addition to mitochondrial membrane potential reduction, we also found that mitochondrial ROS production was elevated in TNFα-treated CATH.a cells, indicative of mitochondrial oxidative injury under inflammatory stress (Fig. 3c, d). However, Mst1 knockdown attenuated mitochondrial ROS overloading, as assessed via flow cytometry (Fig. 3c, d). Moreover, ELISA was used to detect changes in cellular antioxidants. The levels of SOD, GSH, and GPX were rapidly downregulated in response to TNFα (Fig. 3e–g). However, Mst1 knockdown reversed the content of SOD, GSH and GPX in TNFα-treated cells (Fig. 3e–g). Together, the above data indicate that TNFα-mediated mitochondrial oxidative injury and mitochondrial membrane potential reduction could be reversed by Mst1 knockdown.

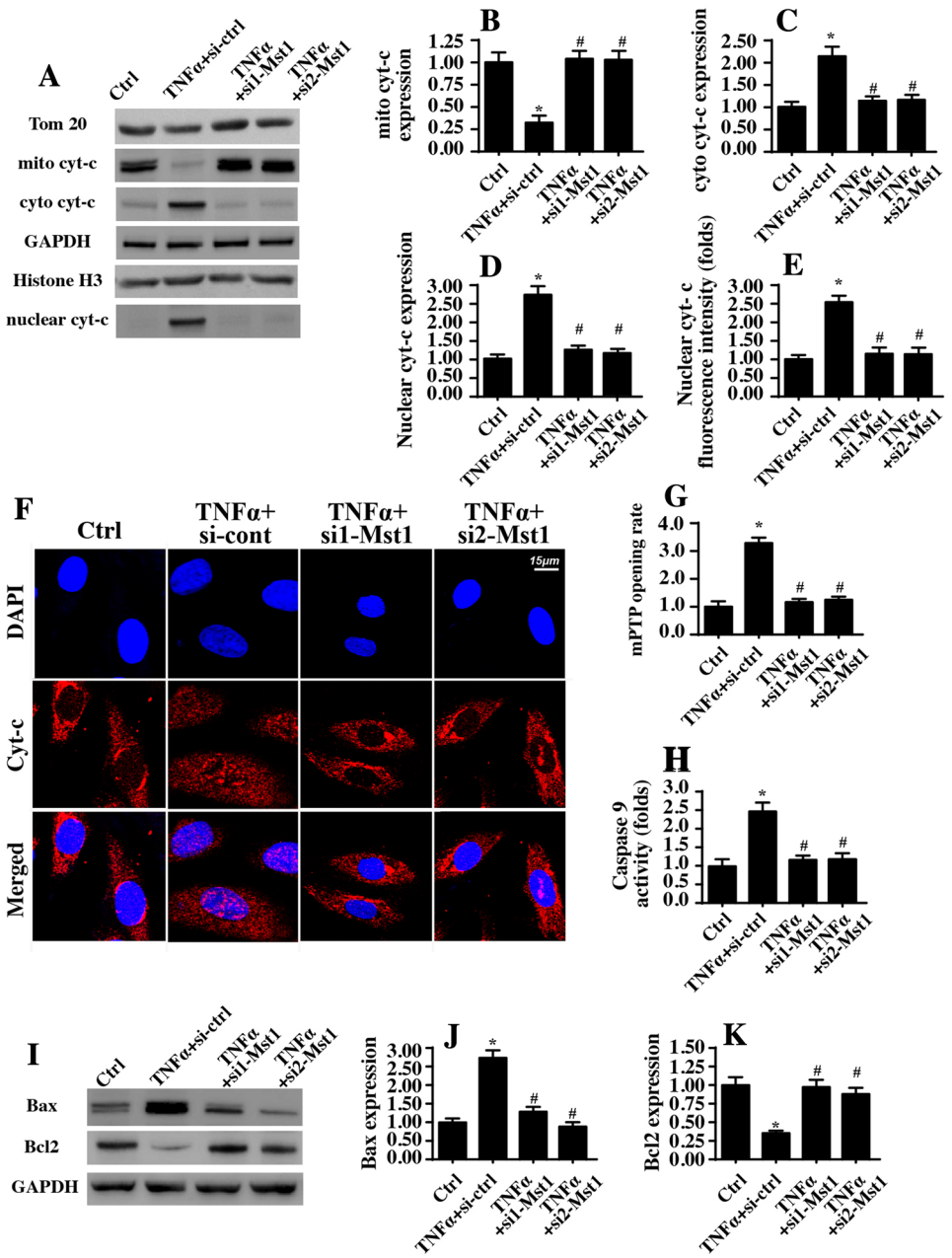

Fig. 2 Mitochondrial apoptosis is activated by TNFα via Mst1. **a**–**d** Proteins were isolated from TNFα-treated CATH.a cells, and the expression of cyt-c was measured using western blot analysis. Tom-20 is the loading control for cytoplasmic cyt-c, and histone H3 is the loading control for nuclear cyt-c. **e**, **f** Immunofluorescence assay for cyt-c. The expression of nuclear cyt-c was determined to reflect the translocation of cyt-c from the cytoplasm into the nucleus. **g** mPTP opening was determined via ELISA. siRNA against Mst1 was used to knockdown Mst1 expression in TNFα-treated CATH.a cells. **h** Caspase-9 activity was measured in CATH.a cells under TNFα treatment and/or Mst1 knockdown. **i**–**k** Proteins were isolated from TNFα-treated CATH.a cells, and then the expression of Bad/Bcl2 was measured using western blot analysis. *p < 0.05 vs. control group; #p < 0.05 vs. TNFα + si-ctrl group

The JNK Pathway is Activated by Inflammatory Injury via Mst1

Subsequently, experiments were conducted to determine the downstream molecular signaling that involves Mst1-mediated cell death and mitochondrial stress. Previous studies have identified the JNK pathway as a potential target of Mst1 in several disease models [46, 47]. In the present study, we investigated the influence of Mst1 on the JNK pathway in TNFα-treated CATH.a cells. As shown in Fig. 4a–c, compared to the control group, the JNK pathway was activated by TNFα treatment, as evidenced by increased p-JNK expression in TNFα-treated CATH.a cells. Interestingly, loss of Mst1 inhibited TNFα-mediated JNK phosphorylation (Fig. 4a–c), indicating that JNK pathway activation is modulated by Mst1. To further demonstrate whether Mst1 was the upstream activator of the JNK pathway, adenovirus-loaded Mst1 was transfected into normal CATH.a cells to perform an Mst1 gain-of-function assay, and then the expression of p-JNK was determined. As shown in Fig. 4a–c, compared to the control group, Mst1 overexpression (Mst1-OE) significantly increased the expression of p-JNK, substantiating the necessity of Mst1 to activate the JNK pathway in CATH.a cells. Subsequently, an immunofluorescence assay was used to observe changes in p-JNK and Mst1 in CATH.a cells. As shown in Fig. 4d–f, compared with that in the control

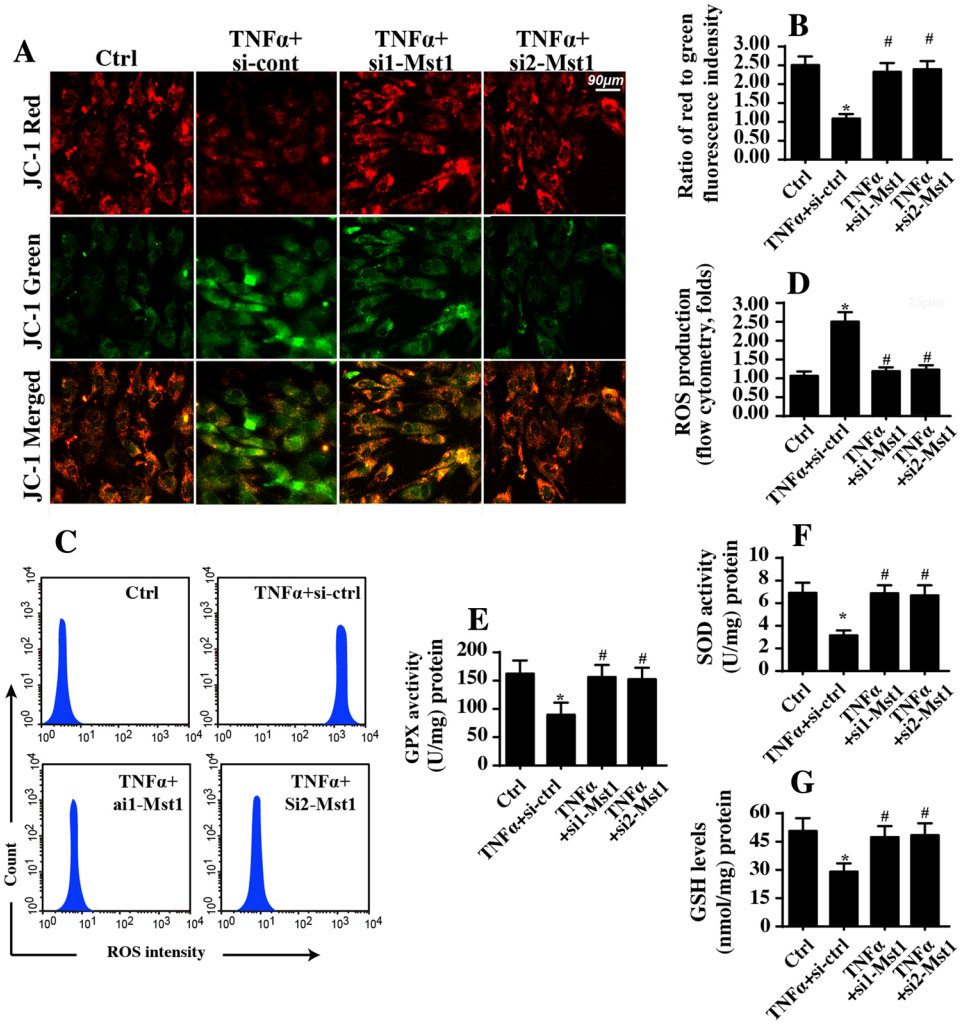

Fig. 3 Mitochondrial function is also modulated by Mst1 under TNFα stress. **a**, **b** Mitochondrial membrane potential was observed via the JC-1 probe. The ratio of red-to-green fluorescence intensity was recorded as a parameter to evaluate mitochondrial membrane potential. **c**, **d** Mitochondrial ROS production was determined via flow cytometry. TNFα treatment elevated ROS generation, and this effect was attenuated by Mst1 knockdown. **e**–**g** As a consequence of mitochondrial oxidative stress, the concentrations of cellular antioxidants were measured via ELISA. *$p < 0.05$ vs. control group; $^{\#}p < 0.05$ vs. TNFα + si-ctrl group

group, the expression of Mst1 was increased, which was followed by an increase in the level of p-JNK. Interestingly, Mst1 knockdown inhibited whereas Mst1-OE increased JNK levels in CATH.a cells, suggesting that Mst1 is required for JNK pathway activation under the TNFα-mediated inflammation response.

Mst1-Activated Mitochondrial Apoptosis is Dependent on the JNK Pathway

Although the JNK pathway is controlled by Mst1, it remains unknown whether the JNK pathway is involved in Mst1-modulated mitochondrial stress in CATH.a cells. To determine the role of the JNK pathway on cell viability and mitochondrial function, a JNK pathway blocker (SP600125) was added to the TNFα-treated cells. Then, mitochondrial function was determined. As shown in Fig. 5a, b, compared to the control group, mitochondrial cyt-c release was activated by TNFα treatment; this effect could be reversed by Mst1 knockdown. Interestingly, inhibition of the JNK pathway also prevented cyt-c translocation into the nucleus (Fig. 5a, b), indicating that mitochondrial pro-apoptotic factor leakage was associated with JNK pathway activation (Fig. 5a, b). In addition, the mPTP opening rate was rapidly increased in TNFα-treated cells and was reversed to near-normal with Mst1 knockdown or SP600125 treatment (Fig. 5c), indicating that JNK inhibition disturbed TNFα-induced mPTP opening. To that end, TNFα-mediated cellular antioxidant downregulation could be reversed by Mst1 knockdown, a result that was similar to that in cells with JNK inhibition (Fig. 5d–f). Therefore, the above data indicate that mitochondrial stress could be ameliorated via inhibiting the JNK pathway under a TNFα-mediated inflammatory response.

Inhibition of JNK Sustains Cell Survival

Lastly, experiments were performed to verify whether the JNK pathway was also associated with cell death induced by TNFα treatment. First, the MTT assay demonstrated that TNFα-mediated CATH.a cell death could be reversed by

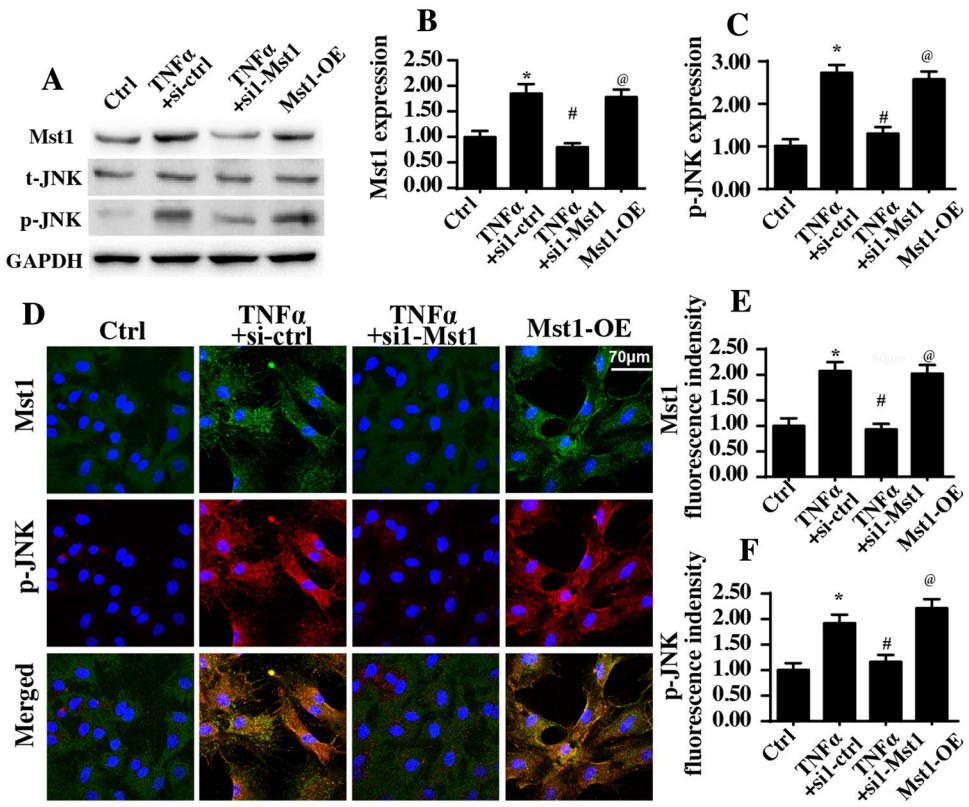

Fig. 4 Increased Mst1 promotes activation of the JNK pathway. **a**–**c** Proteins were isolated from TNFα-treated CATH.a cells, and the expression of p-JNK was measured using western blot analysis. SP600125 was used to inhibit the activation of p-JNK induced by TNFα. siRNA against Mst1 was used to knockdown Mst1 expression in TNFα-treated CATH.a cells. **d**–**f** Immunofluorescence assay for Mst1 and p-JNK. The fluorescence intensities of Mst1 and p-JNK were recorded. SP600125 was used to inhibit the activation of p-JNK induced by TNFα. siRNA against Mst1 was used to knockdown Mst1 expression in TNFα-treated CATH.a cells. *p < 0.05 vs. control group; #p < 0.05 vs. TNFα + si-ctrl group; @p < 0.05 vs. TNFα + si-Mst1 group

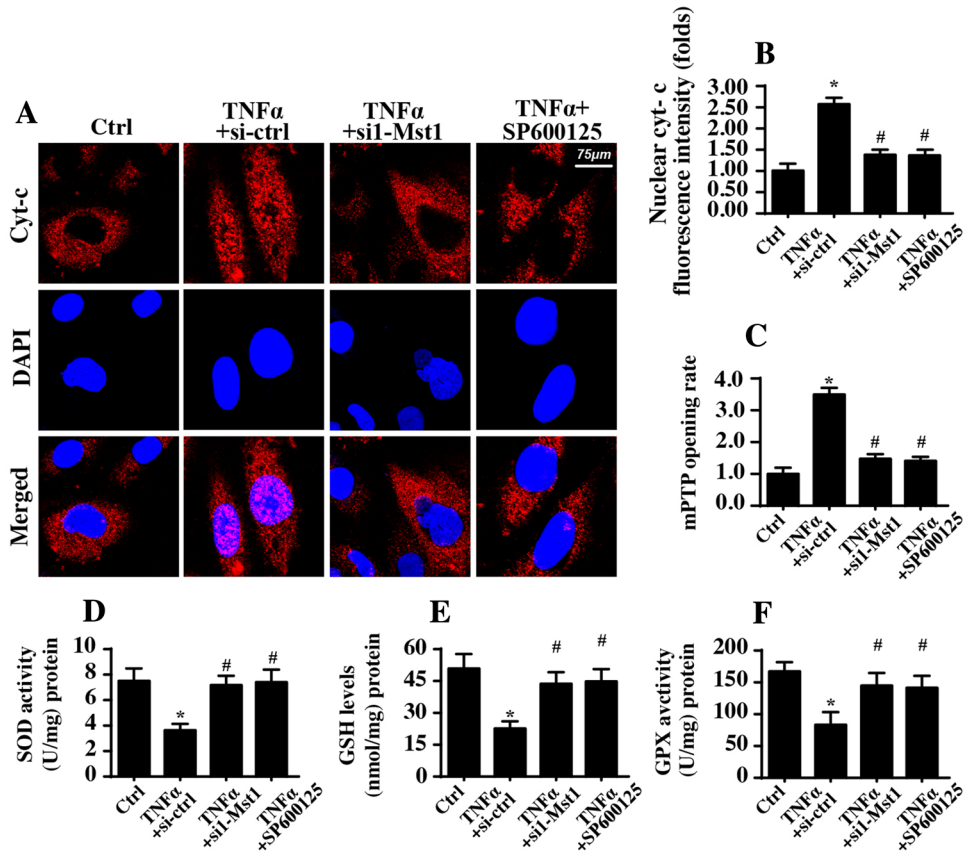

Fig. 5 The JNK pathway is involved in TNFα-mediated mitochondrial apoptosis. **a**, **b** Immunofluorescence assay for cyt-c translocation. SP600125 was used to inhibit the activation of p-JNK induced by TNFα. siRNA against Mst1 was used to knockdown Mst1 expression in TNFα-treated CATH.a cells. **c** mPTP opening was determined via ELISA. **d**–**f** Cellular oxidative stress was evaluated by analyzing the concentration of antioxidants, including SOD, GSH and GPX. *p < 0.05 vs. control group; #p < 0.05 vs. TNFα + si-ctrl group

Mst1 knockdown (Fig. 6a). Moreover, blockade of the JNK pathway also maintained cell viability. This finding was further supported by observing the number of TUNEL-positive cells. As shown in Fig. 6b, c, compared with that in the control group, the percentage of TUNEL-positive CATH.a cells was increased in response to TNFα treatment, where Mst1 knockdown and/or JNK inhibition also repressed the ratio of TUNEL-positive CATH.a cells, reconfirming that the JNK pathway was involved in inflammation-mediated cell death. In addition, western blot analysis demonstrated that the expression of cleaved caspase-3 was upregulated after TNFα treatment and was reduced to near-normal levels with Mst1 knockdown and/or JNK inhibition (Fig. 6d, e). A similar result was also obtained by analyzing the activity of caspase-9 (Fig. 6f). Overall, the above data indicate that the JNK pathway, for which Mst1 is a signaling molecule, plays an essential role in inflammation-mediated CATH.a cell death.

Discussion

Neurodegenerative disorder affects millions of people worldwide, and neuroinflammation has been acknowledged as a primary factor contributing to the pathogenesis of neurodegenerative disease. At the molecular level, inflammation is a complex biological response of the central nervous system to harmful stimuli [48]. Excessive neuroinflammation is associated with necrotic and apoptotic neuronal cell death, which contributes to long-lasting cognitive impairment and motor dysfunction due to functional cell death [49]. In the current study, we found that Mst1 activation would be a novel therapeutic target to control the progression of neuroinflammation and inflammation-mediated neuronal death. Our data illustrated that both Mst1 expression and neuronal apoptosis were significantly elevated in response to TNFα and that knockdown of Mst1 attenuated TNFα-mediated neuronal apoptosis. In addition, we also found that TNFα-mediated neuronal death was accompanied by mitochondrial stress, including mitochondrial oxidative stress, mPTP opening and mitochondrial apoptosis. Furthermore, we provided ample data to support the necessary role played by the JNK pathway in TNFα-mediated neuronal dysfunction and mitochondrial stress. The JNK pathway was activated by TNFα via Mst1, and inhibition of the JNK axis abolished TNFα-mediated neuronal dysfunction and mitochondrial stress in vitro. Altogether, our data identify Mst1–JNK-mitochondrial stress as a new signaling pathway that participates in the progression of neuroinflammation-mediated neuronal death and mitochondrial malfunction. To our knowledge, this is the first study to elucidate the role of the Mst1–JNK-mitochondria cascade in inflammation-mediated neuronal stress. In addition, our findings indicate that Mst1 and mitochondrial stress might be applied as therapeutic targets for the development of new generation treatment agents against neurodegenerative disorders.

Mst1 plays a critical role in regulating cell proliferation, migration, survival and differentiation. The biological

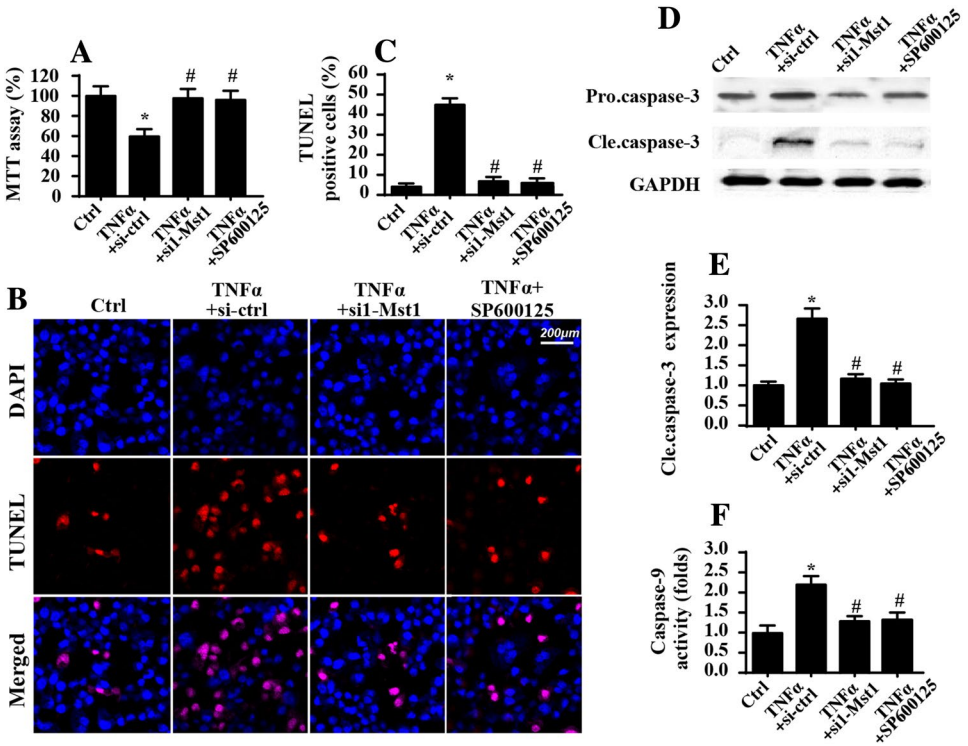

Fig. 6 Cellular apoptosis is modulated by the JNK pathway. **a** Cellular viability was determined via MTT assay. SP600125 was used to inhibit the activation of p-JNK induced by TNFα. siRNA against Mst1 was used to knockdown Mst1 expression in TNFα-treated CATH.a cells. **b**, **c** TUNEL staining for apoptotic cells. The number of apoptotic CATH.a cells was measured in response to TNFα treatment. **d**, **e** Proteins were isolated from TNFα-treated CATH.a cells, and the expression of cleaved caspase-3 was measured using western blot analysis. **f** ELISA was used to measure the changes in caspase-9 activity. *$p < 0.05$ vs. control group; $^{\#}p < 0.05$ vs. TNFα + si-ctrl group

function of Mst1 in the central nervous system has been widely reported. For example, neuron death, spine synapse development, neuronal migration, axon outgrowth, and dendrite growth have been found to be regulated by the Mst1–Hippo pathway [50–53]. In addition, several physiological processes are also affected by Mst1, such as oxidative stress [54], cytoskeletal balance [55], mitochondrial fission [56], mitophagy [57], proinflammatory cytokine release, and IFN-γ-mediated immune response [58]. Accordingly, Mst1 has well-characterized roles in the regulation of various biological functions in the central nervous system. However, the exact actions of Mst1 on neuroinflammation-induced neurodegenerative disease have not been explored. Our current study determined that the inflammatory environment was the upstream trigger of Mst1 and that increased Mst1 was closely linked to neuronal death. This finding further enriches the regulatory mechanism of Mst1 in central nervous system diseases. More importantly, given the potent effects of Mst1 on various pathophysiological biological processes, approaches to affect Mst1 activity would significantly broaden the horizon on potential targets for therapy to treat neuronal diseases.

Recently, mitochondria have been identified as key participants in initiating inflammatory injury, functioning as signaling path-forms and/or downstream effectors. Mitochondria are also the primary targets of several anti-inflammatory therapeutic tools. For example, intracerebral hemorrhage-induced secondary brain injury is associated with an excessive inflammatory response due to mitochondrial dysfunction. In addition, in traumatic brain injury, the NLRP3 inflammasome induces mitochondrial dysfunction and further amplifies the pro-inflammatory response via the release of pro-apoptotic factors into the cytoplasm. Moreover, mitochondrial dysfunction and cellular energy metabolism disorder have been acknowledged as factors in the pathogenesis of Huntington's disease, a severe autosomal dominant neurodegenerative disorder. In the present study, our results also found that mitochondrial damage occurred as a consequence of neuroinflammation due to increased Mst1. Mitochondrial oxidative stress, pro-apoptotic factor release and mPTP opening were noted in TNFα-treated cells. Mitochondrial stress may work together to exacerbate neuronal dysfunction. However, loss of Mst1 sustained mitochondrial function, and mitochondrial protection may help neurons survive under inflammatory conditions. Accordingly, our results provide key insights into the molecular features of mitochondrial stress in neuroinflammation and describe the upstream mediator and downstream event following mitochondrial dysfunction. Therefore, therapeutic interventions that control mitochondrial quality may provide a novel method to treat neuroinflammation.

However, there are several limitations in the present study. First, only cell experiments were performed in the current study, and animal studies are necessary to validate our findings. Second, although we observed Mst1 upregulation in response to neuroinflammation, the molecular mechanism by which inflammation elevates the expression/transcription of Mst1 remains unknown. Together, our results highlight new functions of the Mst1–JNK pathway and mitochondrial stress that are the key mediators of neuroinflammation-mediated neuronal dysfunction.

Authors Contribution CZG, and JCW conceived the research; CZG and CSW performed the experiments; all authors participated in discussing and revising the manuscript.

Data Availability All data generated or analyzed during this study are included in this published article.

Compliance with Ethical Standards

Conflict of interest The authors have declared that they have no conflict of interest.

References

1. Sochocka M, Diniz BS, Leszek J (2017) Inflammatory response in the CNS: friend or foe? Mol Neurobiol 54:8071–8089
2. Ardestani A, Paroni F, Azizi Z, Kaur S, Khobragade V, Yuan T, Frogne T, Tao W, Oberholzer J, Pattou F, Conte JK, Maedler K (2014) MST1 is a key regulator of beta cell apoptosis and dysfunction in diabetes. Nat Med 20:385–397
3. Yao S, Yan W (2018) Overexpression of Mst1 reduces gastric cancer cell viability by repressing the AMPK-Sirt3 pathway and activating mitochondrial fission. Onco Targets Ther 11:8465–8479
4. Qian J, Fang D, Lu H, Cao Y, Zhang J, Ding R, Li L, Huo J (2018) Tanshinone IIA promotes IL2-mediated SW480 colorectal cancer cell apoptosis by triggering INF2-related mitochondrial fission and activating the Mst1–Hippo pathway. Biomed Pharmacother 108:1658–1669
5. Bikfalvi A (2017) History and conceptual developments in vascular biology and angiogenesis research: a personal view. Angiogenesis 20:463–478
6. Blackburn NJR, Vulesevic B, McNeill B, Cimenci CE, Ahmadi A, Gonzalez-Gomez M, Ostojic A, Zhong Z, Brownlee M, Beisswenger PJ, Milne RW, Suuronen EJ (2017) Methylglyoxal-derived advanced glycation end products contribute to negative cardiac remodeling and dysfunction post-myocardial infarction. Basic Res Cardiol 112:57
7. Abdulmahdi W, Patel D, Rabadi MM, Azar T, Jules E, Lipphardt M, Hashemiyoon R, Ratliff BB (2017) HMGB1 redox during sepsis. Redox Biol 13:600–607
8. Brazao V, Santello FH, Colato RP, Mazotti TT, Tazinafo LF, Toldo MPA, do Vale GT, Tirapelli CR, do Prado JC Jr (2017) Melatonin: antioxidant and modulatory properties in age-related changes during *Trypanosoma cruzi* infection. J Pineal Res 63:e12409
9. Buijs N, Oosterink JE, Jessup M, Schierbeek H, Stolz DB, Houdijk AP, Geller DA, van Leeuwen PA (2017) A new key player in VEGF-dependent angiogenesis in human hepatocellular carcinoma: dimethylarginine dimethylaminohydrolase 1. Angiogenesis 20:557–565

10. Casadonte L, Verhoeff BJ, Piek JJ, VanBavel E, Spaan JAE, Siebes M (2017) Influence of increased heart rate and aortic pressure on resting indices of functional coronary stenosis severity. Basic Res Cardiol 112:61
11. Antunes F, Brito PM (2017) Quantitative biology of hydrogen peroxide signaling. Redox Biol 13:1–7
12. Conradi LC, Brajic A, Cantelmo AR, Bouche A, Kalucka J, Pircher A, Bruning U, Teuwen LA, Vinckier S, Ghesquiere B, Dewerchin M, Carmeliet P (2017) Tumor vessel disintegration by maximum tolerable PFKFB3 blockade. Angiogenesis 20:599–613
13. Chang SH, Yeh YH, Lee JL, Hsu YJ, Kuo CT, Chen WJ (2017) Transforming growth factor-beta-mediated CD44/STAT3 signaling contributes to the development of atrial fibrosis and fibrillation. Basic Res Cardiol 112:58
14. Zhang M, Lin J, Wang S, Cheng Z, Hu J, Wang T, Man W, Yin T, Guo W, Gao E, Reiter RJ, Wang H, Sun D (2017) Melatonin protects against diabetic cardiomyopathy through Mst1/Sirt3 signaling. J Pineal Res 63:e12418
15. Fukumoto M, Kondo K, Uni K, Ishiguro T, Hayashi M, Ueda S, Mori I, Niimi K, Tashiro F, Miyazaki S, Miyazaki JI, Inagaki S, Furuyama T (2018) Tip-cell behavior is regulated by transcription factor FoxO1 under hypoxic conditions in developing mouse retinas. Angiogenesis 21:203–214
16. Li H, Feng J, Zhang Y, Feng J, Wang Q, Zhao S, Meng P, Li J (2019) Mst1 deletion attenuates renal ischaemia-reperfusion injury: the role of microtubule cytoskeleton dynamics, mitochondrial fission and the GSK3beta-p53 signalling pathway. Redox Biol 20:261–274
17. Cohen MV, Downey JM (2017) The impact of irreproducibility and competing protection from P2Y12 antagonists on the discovery of cardioprotective interventions. Basic Res Cardiol 112:64
18. Chen T, Dai SH, Li X, Luo P, Zhu J, Wang YH, Fei Z, Jiang XF (2018) Sirt1-Sirt3 axis regulates human blood-brain barrier permeability in response to ischemia. Redox Biol 14:229–236
19. Brazao V, Colato RP, Santello FH, Vale GTD, Gonzaga NA, Tirapelli CR, Prado JCD Jr (2018) Effects of melatonin on thymic and oxidative stress dysfunctions during *Trypanosoma cruzi* infection. J Pineal Res 65:e12510
20. Zhou H, Shi C, Hu S, Zhu H, Ren J, Chen Y (2018) BI1 is associated with microvascular protection in cardiac ischemia reperfusion injury via repressing Syk-Nox2-Drp1-mitochondrial fission pathways. Angiogenesis 21:599–615
21. Gonzalez NR, Liou R, Kurth F, Jiang H, Saver J (2018) Antiangiogenesis and medical therapy failure in intracranial atherosclerosis. Angiogenesis 21:23–35
22. Hong H, Tao T, Chen S, Liang C, Qiu Y, Zhou Y, Zhang R (2017) MicroRNA-143 promotes cardiac ischemia-mediated mitochondrial impairment by the inhibition of protein kinase Cepsilon. Basic Res Cardiol 112:60
23. Cai SY, Zhang Y, Xu YP, Qi ZY, Li MQ, Ahammed GJ, Xia XJ, Shi K, Zhou YH, Reiter RJ, Yu JQ, Zhou J (2017) HsfA1a upregulates melatonin biosynthesis to confer cadmium tolerance in tomato plants. J Pineal Res 62:e12387
24. Hassanshahi M, Hassanshahi A, Khabbazi S, Su YW, Xian CJ (2017) Bone marrow sinusoidal endothelium: damage and potential regeneration following cancer radiotherapy or chemotherapy. Angiogenesis 20:427–442
25. Hooshdaran B, Kolpakov MA, Guo X, Miller SA, Wang T, Tilley DG, Rafiq K, Sabri A (2017) Dual inhibition of cathepsin G and chymase reduces myocyte death and improves cardiac remodeling after myocardial ischemia reperfusion injury. Basic Res Cardiol 112:62
26. Das N, Mandala A, Naaz S, Giri S, Jain M, Bandyopadhyay D, Reiter RJ, Roy SS (2017) Melatonin protects against lipid-induced mitochondrial dysfunction in hepatocytes and inhibits stellate cell activation during hepatic fibrosis in mice. J Pineal Res 62:e12404
27. Zhou H, Wang J, Zhu P, Zhu H, Toan S, Hu S, Ren J, Chen Y (2018) NR4A1 aggravates the cardiac microvascular ischemia reperfusion injury through suppressing FUNDC1-mediated mitophagy and promoting Mff-required mitochondrial fission by CK2alpha. Basic Res Cardiol 113:23
28. Galley HF, McCormick B, Wilson KL, Lowes DA, Colvin L, Torsney C (2017) Melatonin limits paclitaxel-induced mitochondrial dysfunction in vitro and protects against paclitaxel-induced neuropathic pain in the rat. J Pineal Res 63:e12444
29. Hatori Y, Inouye S, Akagi R, Seyama T (2018) Local redox environment beneath biological membranes probed by palmitoylated-roGFP. Redox Biol 14:679–685
30. Cortese-Krott MM, Mergia E, Kramer CM, Luckstadt W, Yang J, Wolff G, Panknin C, Bracht T, Sitek B, Pernow J, Stasch JP, Feelisch M, Koesling D, Kelm M (2018) Identification of a soluble guanylate cyclase in RBCs: preserved activity in patients with coronary artery disease. Redox Biol 14:328–337
31. Carloni S, Riparini G, Buonocore G, Balduini W (2017) Rapid modulation of the silent information regulator 1 by melatonin after hypoxia-ischemia in the neonatal rat brain. J Pineal Res 63:e12434
32. Kelly P, Denver P, Satchell SC, Ackermann M, Konerding MA, Mitchell CA (2017) Microvascular ultrastructural changes precede cognitive impairment in the murine APPswe/PS1dE9 model of Alzheimer's disease. Angiogenesis 20:567–580
33. Koentges C, Pepin ME, Musse C, Pfeil K, Alvarez SVV, Hoppe N, Hoffmann MM, Odening KE, Sossalla S, Zirlik A, Hein L, Bode C, Wende AR, Bugger H (2017) Gene expression analysis to identify mechanisms underlying heart failure susceptibility in mice and humans. Basic Res Cardiol 113:8
34. Dominguez-Rodriguez A, Abreu-Gonzalez P, de la Torre-Hernandez JM, Gonzalez-Gonzalez J, Garcia-Camarero T, Consuegra-Sanchez L, Garcia-Saiz MD, Aldea-Perona A, Virgos-Aller T, Azpeitia A, Reiter RJ (2017) Effect of intravenous and intracoronary melatonin as an adjunct to primary percutaneous coronary intervention for acute ST-elevation myocardial infarction: results of the melatonin adjunct in the acute myocardial infarction treated with angioplasty trial. J Pineal Res 62:e12374
35. Yuan F, Xie Q, Wu J, Bai Y, Mao B, Dong Y, Bi W, Ji G, Tao W, Wang Y, Yuan Z (2011) MST1 promotes apoptosis through regulating Sirt1-dependent p53 deacetylation. J Biol Chem 286:6940–6945
36. Jin Q, Li R, Hu N, Xin T, Zhu P, Hu S, Ma S, Zhu H, Ren J, Zhou H (2018) DUSP1 alleviates cardiac ischemia/reperfusion injury by suppressing the Mff-required mitochondrial fission and Bnip3-related mitophagy via the JNK pathways. Redox Biol 14:576–587
37. Liu Z, Liu Y, Xu Q, Peng H, Tang Y, Yang T, Yu Z, Cheng G, Zhang G, Shi R (2017) Critical role of vascular peroxidase 1 in regulating endothelial nitric oxide synthase. Redox Biol 12:226–232
38. Camare C, Pucelle M, Negre-Salvayre A, Salvayre R (2017) Angiogenesis in the atherosclerotic plaque. Redox Biol 12:18–34
39. Gao L, Zhao YC, Liang Y, Lin XH, Tan YJ, Wu DD, Li XZ, Ye BZ, Kong FQ, Sheng JZ, Huang HF (2016) The impaired myocardial ischemic tolerance in adult offspring of diabetic pregnancy is restored by maternal melatonin treatment. J Pineal Res 61:340–352
40. Fan T, Pi H, Li M, Ren Z, He Z, Zhu F, Tian L, Tu M, Xie J, Liu M, Li Y, Tan M, Li G, Qing W, Reiter RJ, Yu Z, Wu H, Zhou Z (2018) Inhibiting MT2-TFE3-dependent autophagy enhances melatonin-induced apoptosis in tongue squamous cell carcinoma. J Pineal Res 64:e12457
41. Zhou H, Zhu P, Wang J, Zhu H, Ren J, Chen Y (2018) Pathogenesis of cardiac ischemia reperfusion injury is associated with CK2alpha-disturbed mitochondrial homeostasis via suppression of FUNDC1-related mitophagy. Cell Death Differ 25:1080–1093

42. Nawaz IM, Chiodelli P, Rezzola S, Paganini G, Corsini M, Lodola A, Di Ianni A, Mor M, Presta M (2018) N-tert-butyloxycarbonyl-Phe-Leu-Phe-Leu-Phe (BOC2) inhibits the angiogenic activity of heparin-binding growth factors. Angiogenesis 21:47–59
43. Li W, Chen X, Riley AM, Hiett SC, Temm CJ, Beli E, Long X, Chakraborty S, Alloosh M, White FA, Grant MB, Sturek M, Obukhov AG (2017) Long-term spironolactone treatment reduces coronary TRPC expression, vasoconstriction, and atherosclerosis in metabolic syndrome pigs. Basic Res Cardiol 112:54
44. Dickinson JD, Sweeter JM, Warren KJ, Ahmad IM, De Deken X, Zimmerman MC, Brody SL (2018) Autophagy regulates DUOX1 localization and superoxide production in airway epithelial cells during chronic IL-13 stimulation. Redox Biol 14:272–284
45. Zhou H, Zhu P, Guo J, Hu N, Wang S, Li D, Hu S, Ren J, Cao F, Chen Y (2017) Ripk3 induces mitochondrial apoptosis via inhibition of FUNDC1 mitophagy in cardiac IR injury. Redox Biol 13:498–507
46. Ganini D, Leinisch F, Kumar A, Jiang J, Tokar EJ, Malone CC, Petrovich RM, Mason RP (2017) Fluorescent proteins such as eGFP lead to catalytic oxidative stress in cells. Redox Biol 12:462–468
47. Rossello X, Riquelme JA, He Z, Taferner S, Vanhaesebroeck B, Davidson SM, Yellon DM (2017) The role of PI3Kalpha isoform in cardioprotection. Basic Res Cardiol 112:66
48. Pryds K, Nielsen RR, Jorsal A, Hansen MS, Ringgaard S, Refsgaard J, Kim WY, Petersen AK, Botker HE, Schmidt MR (2017) Effect of long-term remote ischemic conditioning in patients with chronic ischemic heart failure. Basic Res Cardiol 112:67
49. Turner CJ, Badu-Nkansah K, Hynes RO (2017) Endothelium-derived fibronectin regulates neonatal vascular morphogenesis in an autocrine fashion. Angiogenesis 20:519–531
50. Lee HY, Back K (2017) Melatonin is required for H^2O^{2-} and NO-mediated defense signaling through MAPKKK3 and OXI1 in *Arabidopsis thaliana*. J Pineal Res 62:e12379
51. Koka S, Xia M, Chen Y, Bhat OM, Yuan X, Boini KM, Li PL (2017) Endothelial NLRP3 inflammasome activation and arterial neointima formation associated with acid sphingomyelinase during hypercholesterolemia. Redox Biol 13:336–344
52. Zhou J, Zhang H, Wang H, Lutz AM, El Kaffas A, Tian L, Hristov D, Willmann JK (2017) Early prediction of tumor response to bevacizumab treatment in murine colon cancer models using three-dimensional dynamic contrast-enhanced ultrasound imaging. Angiogenesis 20:547–555
53. Schulz R, Agg B, Ferdinandy P (2017) Survival pathways in cardiac conditioning: individual data vs. meta-analyses. What do we learn? Basic Res Cardiol 113:4
54. Jang H, Na Y, Hong K, Lee S, Moon S, Cho M, Park M, Lee OH, Chang EM, Lee DR, Ko JJ, Lee WS, Choi Y (2017) Synergistic effect of melatonin and ghrelin in preventing cisplatin-induced ovarian damage via regulation of FOXO3a phosphorylation and binding to the p27(Kip1) promoter in primordial follicles. J Pineal Res 63:e12432
55. Morell M, Burgos JI, Gonano LA, Vila Petroff M (2017) AMPK-dependent nitric oxide release provides contractile support during hyperosmotic stress. Basic Res Cardiol 113:7
56. Espinosa-Diez C, Miguel V, Vallejo S, Sanchez FJ, Sandoval E, Blanco E, Cannata P, Peiro C, Sanchez-Ferrer CF, Lamas S (2018) Role of glutathione biosynthesis in endothelial dysfunction and fibrosis. Redox Biol 14:88–99
57. van Beijnum JR, Nowak-Sliwinska P, van Berkel M, Wong TJ, Griffioen AW (2017) A genomic screen for angiosuppressor genes in the tumor endothelium identifies a multifaceted angiostatic role for bromodomain containing 7 (BRD7). Angiogenesis 20:641–654
58. Li Z, Li X, Chen C, Chan MTV, Wu WKK, Shen J (2017) Melatonin inhibits nucleus pulposus (NP) cell proliferation and extracellular matrix (ECM) remodeling via the melatonin membrane receptors mediated PI3K-Akt pathway. J Pineal Res 63:e12435